Supporting Information for

Self-Assembled D-π-A multifunctional systems with tunable Stimuli-Responsive Emission and Optical Waveguiding Behaviour

R. Martín,[a,b†] A. Sánchez-Oliva,[b†] A. Benito,[a] I. Torres-Moya,[b,c] A. M. García,[b] J. Álvarez-Conde,[d] J. Cabanillas-González, [*d] P. Prieto,[*b] B. Gómez-Lor.[*a]

a) Institute of Materials Science of Madrid (ICMM-CSIC), Sor Juana Inés de la Cruz 3, Cantoblanco 28049, Madrid, Spain.
E-mail: bgl@icmm.csic.es
b) Faculty of Chemical Science and Technology, University of Castilla-La Mancha, Instituto Regional de Investigación Científica Aplicada (IRICA), University of Castilla-La Mancha, 13071 Ciudad Real, Spain.
E-mail: Mariapilar.Prieto@uclm.es
c) Department of Organic Chemistry, Faculty of Chemical Sciences, Campus of Espinardo, University of Murcia. 30100 Murcia, Spain.
d) Madrid Institute for Advanced Studies, IMDEA Nanociencia, Calle Faraday 9, Cantoblanco, 28049, Madrid, Spain.
E-mail: juan.cabanillas@imdea.org

†These authors contributed equally to this work.

CONTENT

1. Experimental details

All reagents were used as purchased. Reactions with air-sensitive materials were carried out under an argon atmosphere.

Microwave reactor: Reactions under microwave irradiation were performed in a Discover® (CEM) focused microwave reactor. Measurements and temperature control were performed with an infrared reader and parameters were recorded using the program designed by CEM.

Nuclear Magnetic Resonance (NMR) characterization: ^{1}H-NMR and ^{13}C-NMR spectra were recorded on a Varian Unity 500 (^{1}H 500 MHz; ^{13}C 125 MHz) spectrometer at 298 K using partially deuterated solvents as internal reference. Coupling constants (*J*) are denoted in Hz and chemical shifts (d in ppm. Multiplicities are denoted as: s = singlet, d = doublet, t = triplet, m = multiplet, br = broad).

Mass spectrometry: MALDI-TOF mass spectra were obtained on a Bruker Autoflex II TOF/TOF spectrometer (Bremen, Germany) using dithranol as the matrix. Samples, co-crystallized with the matrix on the probe, were ionized with a nitrogen laser pulse (337 nm) and accelerated under 20 kV with time-delayed extraction before entering the time-of-flight mass spectrometer. Matrix (10 mg/mL) and sample (1 mg/mL) were separately dissolved in methanol and mixed in a matrix/sample ratio ranging from 100:1 to 50:1. Typically, a 5 µL mixture of matrix and sample was applied to a MALDI-TOF MS probe and air-dried. MALDITOF MS in positive reflector mode was used for all samples. External calibration was performed by using Peptide Calibration Standard II (covered mass range: 700–3200 Da) from Care (Bruker). The applied peak (*m*/*z* determination) detection method was the threshold centroid at 50% height of the peak maximum.

Linear Spectroscopy: UV-Vis spectra were recorded on a Varian Cary model 5000 UV-Vis-NIR spectrophotometer using standard quartz cells of 1 cm width and solvents of spectroscopic grade and PerkinElmer Lambda XLS+ spectrometer. Fluorescence spectra were recorded on an Aminco SLM 8000 spectrophotometer.

Scanning Electron Microscope: Scanning Electron Microscope (SEM) images were obtained on a JEOL JSM 6335F microscope working at 10 kV. The samples for SEM

imaging were prepared by a controlled precipitation using the appropriate solvent or by slow diffusion by using mixtures of solvents, depending on their solubility properties. The corresponding solid was deposited onto a glass substrate and the remaining solvent was slowly evaporated.

Optical waveguide behaviour: PL microscopy images for crystal needles were acquired with a Nikon Eclipse Ti inverted microscope with dry objectives (100X N.A. 0.8 and 20X N.A. 0.45) coupled to a Shamrock spectrometer from Andor Technology with a thermoelectrically cooled Newton EM (Andor) CCD. The excitation was obtained by appropriate filtering of the lines from a Xe lamp.

Loss coefficients in crystals were obtained upon exciting them with a pulsed Nd:YAG laser (355 nm, 300 ps, 1 KHz, 30 μJ/pulse). A set of filters were employed to attenuate the photoexcitation. Detection from the crystal edge was focused in free space on to a 0.5 m length SP2558 Princeton Instruments (Acton Research) spectrometer equipped with a 600 lines/mm grating and a liquid nitrogen cooled CCD.

Powder X-ray diffraction: Powder X-ray diffraction (PXRD) patterns were measured with a Bruker D8 diffractometer, with step size = 0.02° and exposure time = 0.5 s/step.

Product purification: Flash chromatography was performed using silica gel (Merck, Kieselgel 60, 230–240 mesh or Scharlau 60, 230–240 mesh). Analytical thin layer chromatography (TLC) was performed to follow the reaction by using aluminium-coated Merck Kieselgel 60 F254 plates.

X-ray diffraction: Crystals of **NI1** and **NI2** were solved in a XtaLAB Synergy R, HyPix-Arc 100 diffractometer.

Thin film thickness: The thin film thickness was measured with a Profilm3D optical profilometer employing white light interferometry (WLI).

Thermogravimetric Analysis (TGA): TGA measurements were performed using a TA Instruments Q500 thermobalance equipped with an EGA furnace. Pt and N_2 sample holders were employed as purge gas with a flow rate of 90 mL/min. The samples were heated from room temperature to 800°C.

Differential Scanning Calorimetry (DSC): DSC curves were recorded on a TA Instruments Discovery DSC calorimeter, utilizing standard TzeroTM sample holders. The purge gas used was N_2 at a flow rate of 50 mL/min, and a heating ramp of 10ºC/min from -50 °C to 200 °C was applied.

2. ^{1}H-NMR, ^{13}C-NMR and MS spectra.

Compound 2a

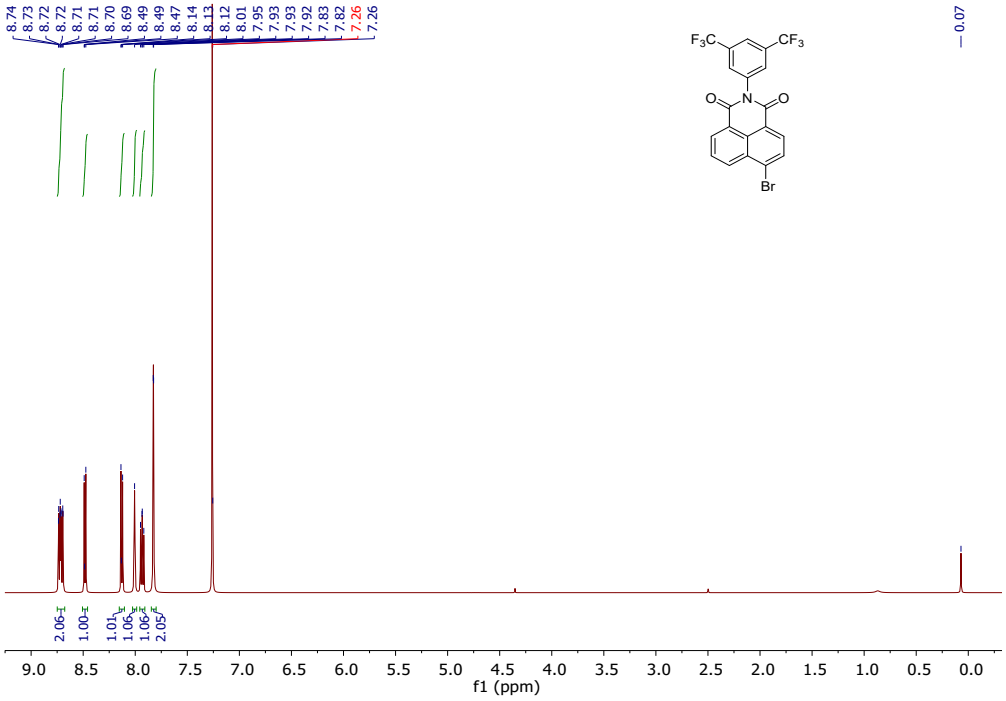

Figure S1. ^{1}H-NMR spectrum of **2a**.

Compound 2b

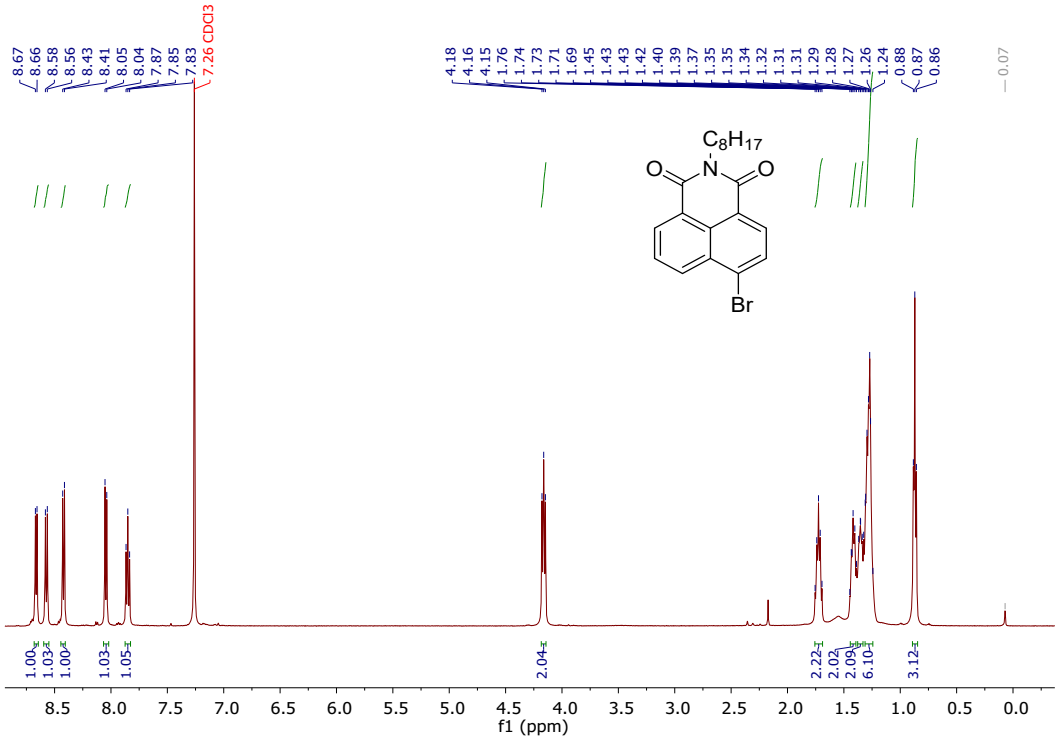

Figure S2. ^{1}H-NMR spectrum of **2b**.

Compound NI1

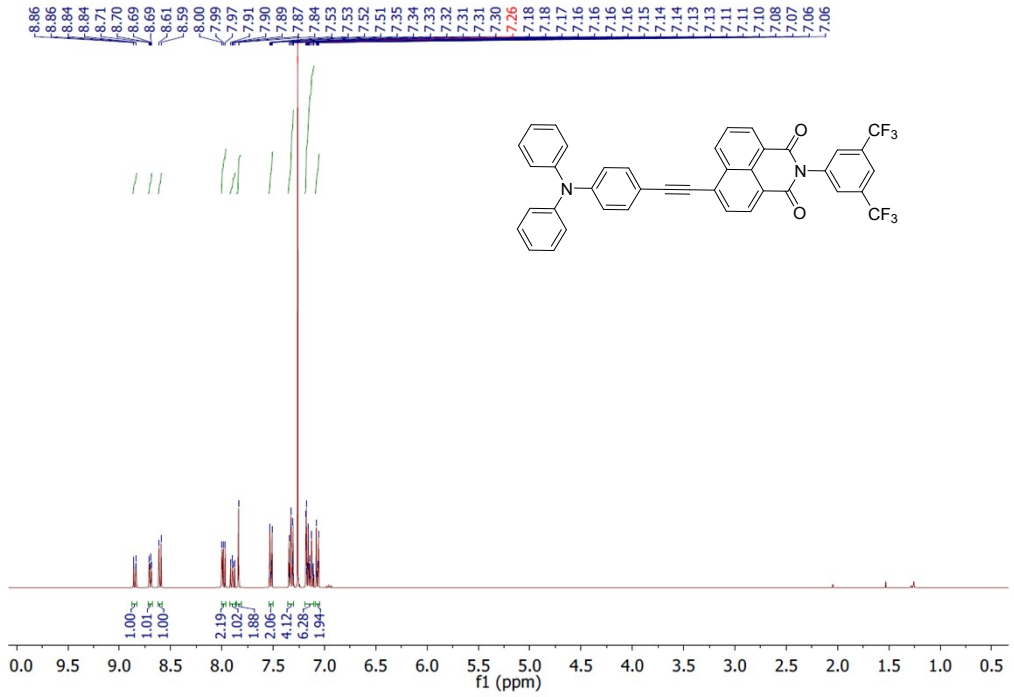

Figure S3. ^{1}H-NMR spectrum of **NI1**.

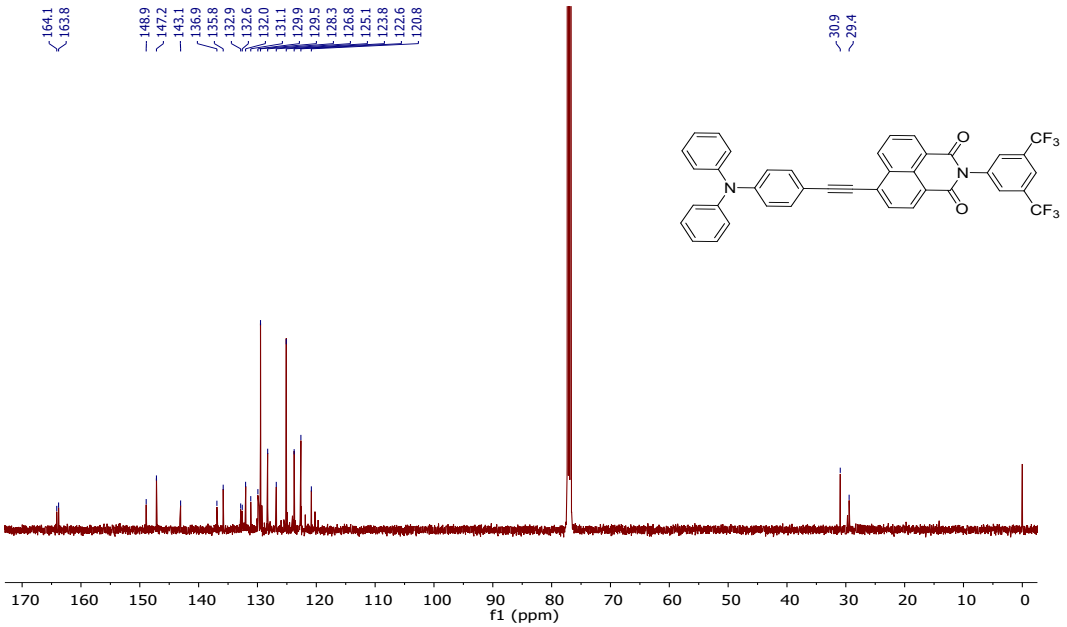

Figure S4. ^{13}C-NMR spectrum of **NI1**.

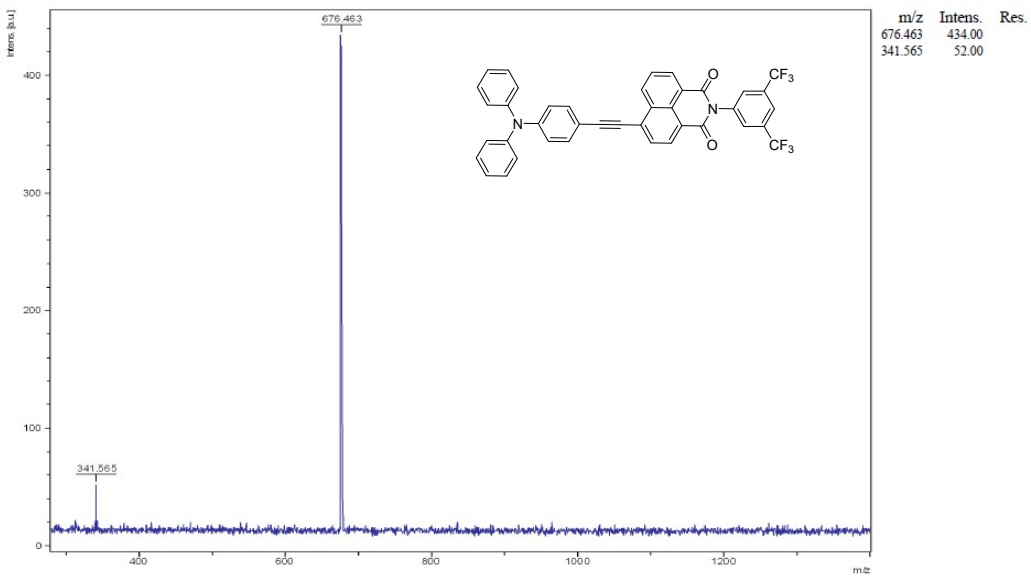

Figure S5. Mass spectrum of **NI1**.

3. SEM images

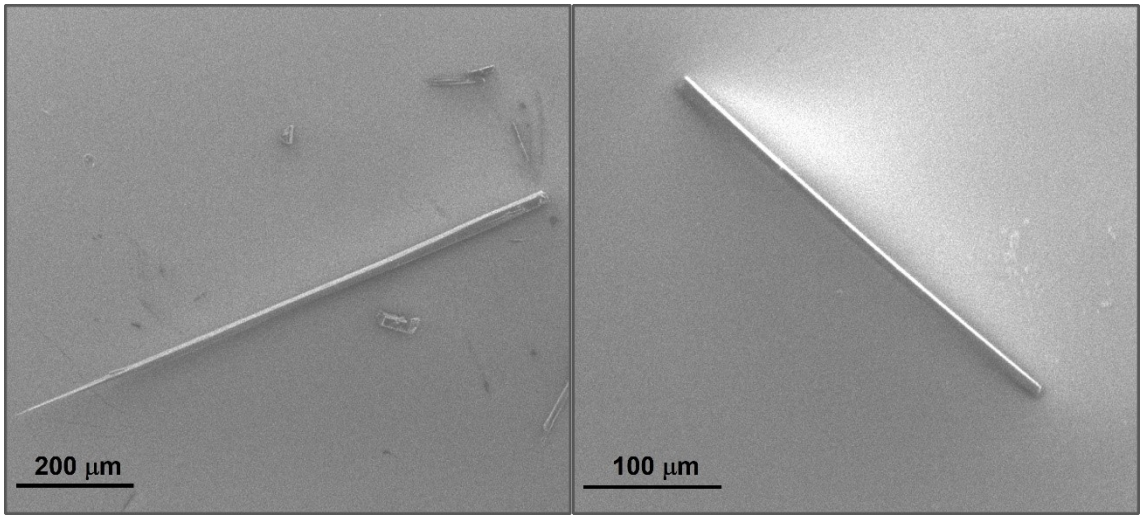

Figure S6. SEM images of crystals formed by **NI1** in THF/hexane.

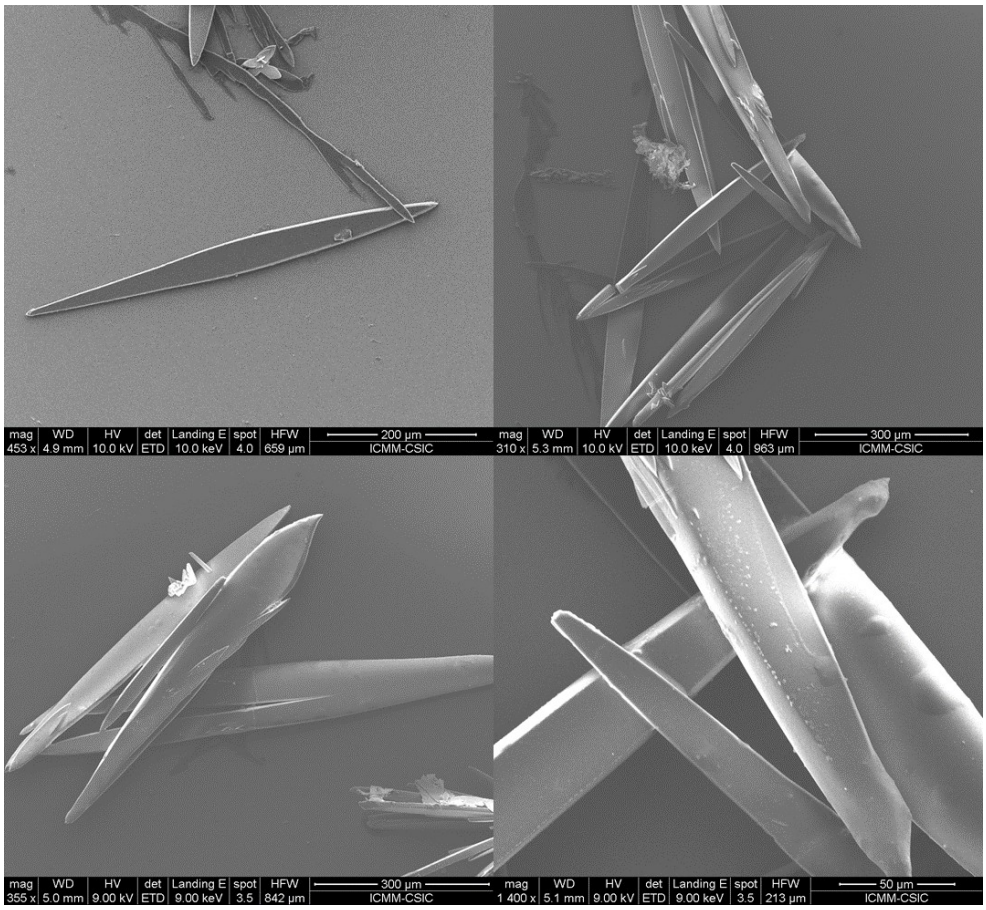

Figure S7. SEM images for the crystals formed by **NI2** in THF/CH_3OH.

4. Optical waveguide measurement

The optical loss coefficients were measured following the set up described in Figure S8. The measurement relied on the loss of collected light as the photoexcitation spot is moved away from the waveguide exit (tip). The photoexcitation was provided by a pulsed Nd:YAG laser (355, 300 ps, 1KHz, 30 µJ/pulse). The fluence was controlled by a variable density filters and redirected by a UV mirror to a cylindrical lens to convert the laser beam into a narrow stripe 400 µm x 4 mm aligned perpendicular to the organic fiber. The emission of the tip of the fiber is collected in a free-space configuration Just before the spectrometer, a long pass filter was placed to cut off reflected excitation-

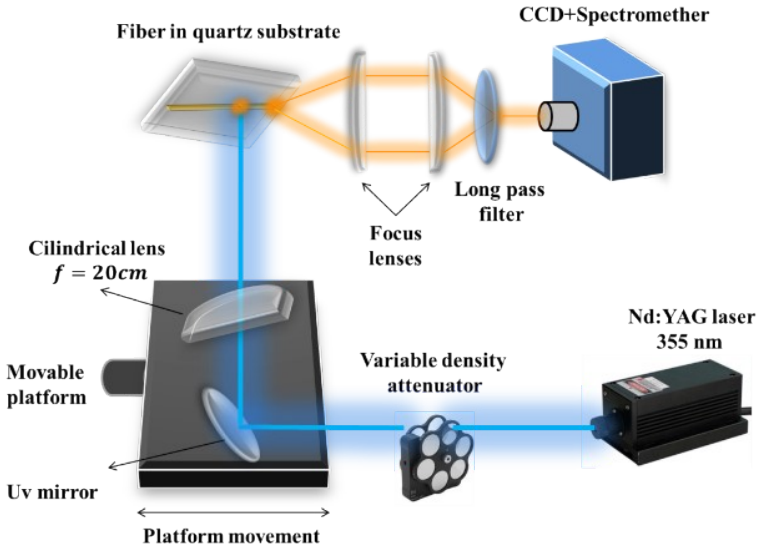

Figure S8. Schematic representation of the set-up used for the measurement of optical loss of **NI1** and **NI2**.

5. Photophysical characterization

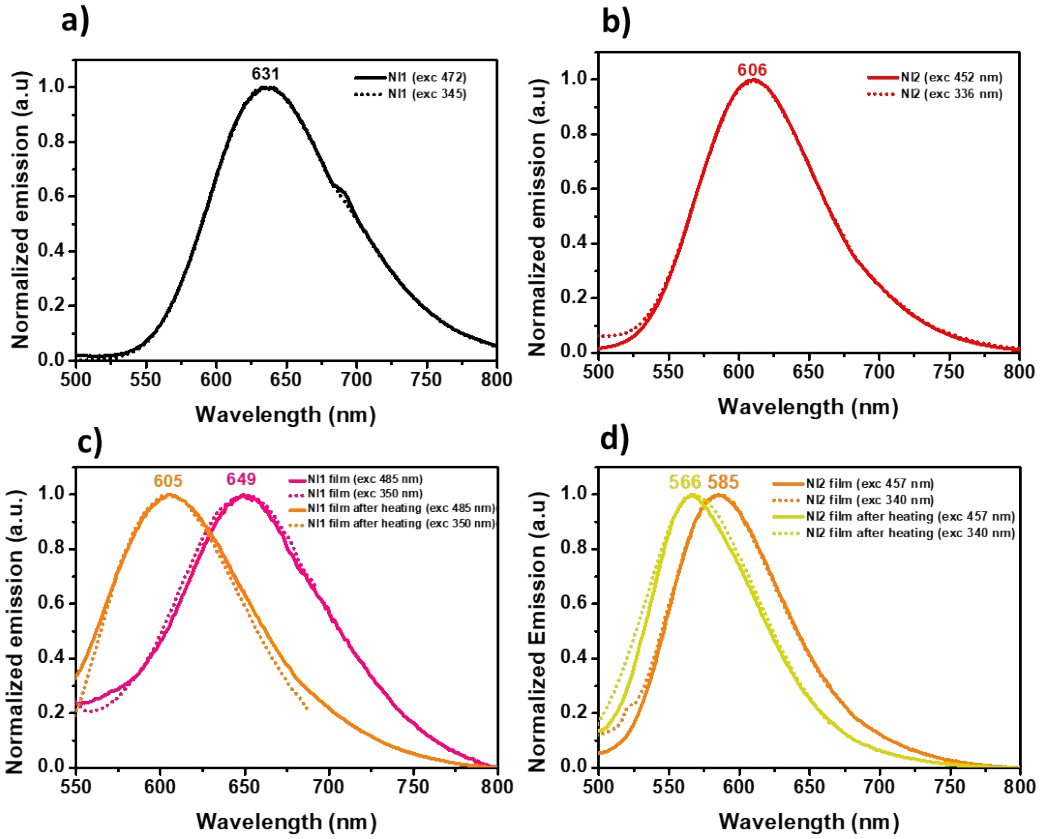

Figure S9. Comparison of the emission spectra of NI compounds in solution ($CHCl_3$, $1 \cdot 10^{-5}$ M) (a,b) and in the thin films (c,d) after excitation at the π-π* and ICT absorption bands.

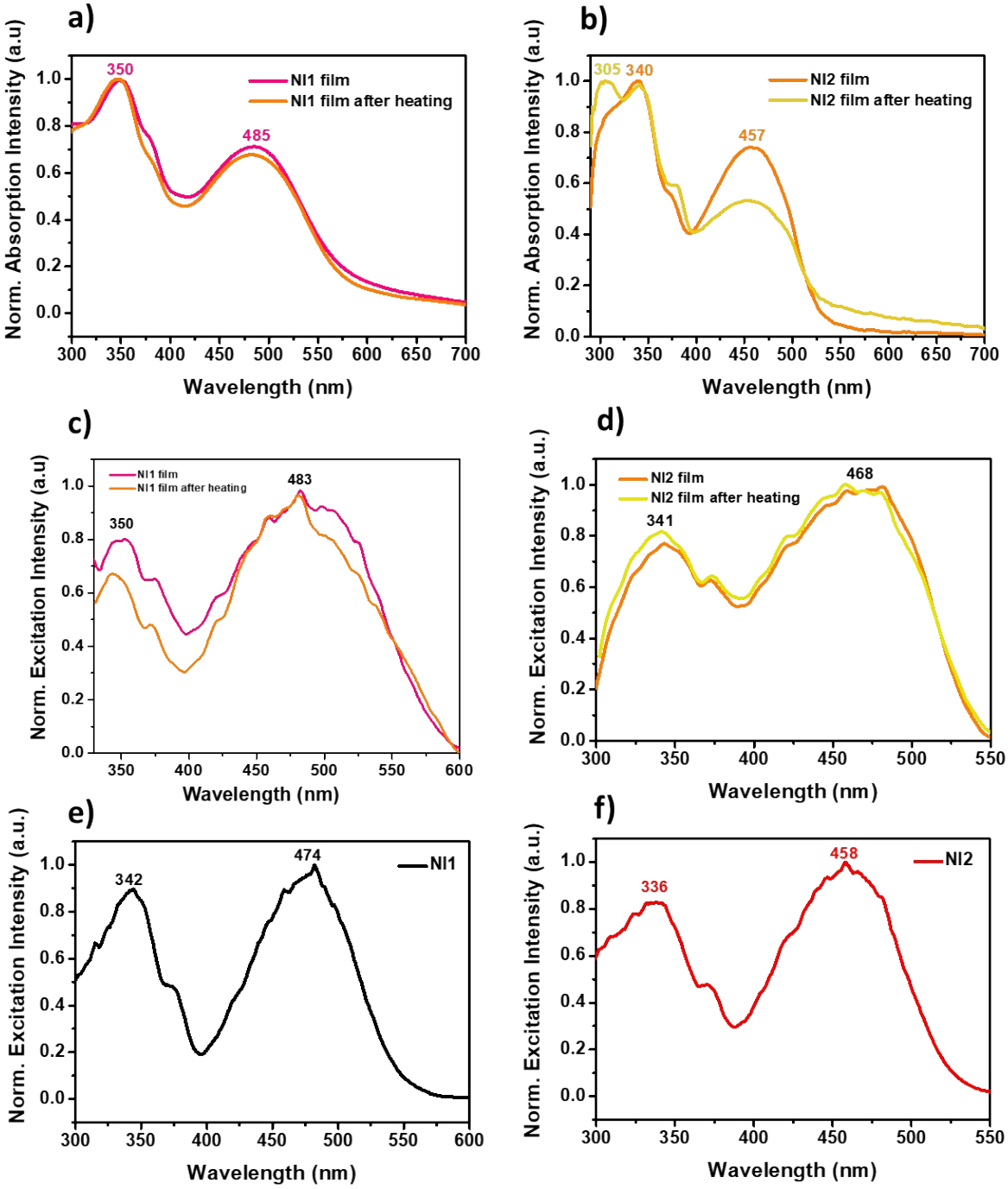

Figure S10. Absorption spectra of the thin film layers for a) **NI1** and b) **NI2** and excitation spectra of c) **NI1** and d) **NI2** in the thin layers and e) **NI1** and f) **NI2** in the solution

Photoluminescence Lifetimes

Both **N1** and **N2** in they amorphous and crystalline forms, show multiexponential decays that require 3 or 4 components to be fitted. Intensity-weighted average tau values (calculated according to equation 1) for **N1** in its amorphous and crystalline forms are 4.18 ns and 3.27 ns, while the corresponding tau values for **N2** in its amorphous and crystalline form are 5.09 ns and 10.11 ns respectively.

In general, multi-exponential PL decay indicates the presence of non-radiative decay channels competing with emission, either located within the molecules or via the interplay of different molecules. Examples are dynamic quenching processes which require exciton diffusion, such as exciton annihilation phenomena or exciton trapping at crystal defects or boundaries. These phenomena give rise to depopulation of excited states with different rates, leading to the characteristic non-exponential behaviour [1].

$$\tau_{Av\,Int} = \sum_{\substack{i=1 \\ I_i>0}}^{n_{Exp}} I_i \tau_i \Big/ \sum_{\substack{i=1 \\ I_i>0}}^{n_{Exp}} I_i$$

Equation 1

a)

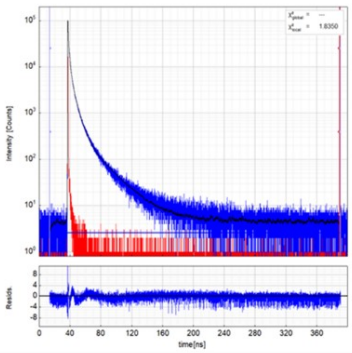

Parameter	Value	Δ	δ
A_1[kCnts/Chnl]	0.414	±0.033	7.9%
τ_1[ns]	21.93	±0.59	2.7%
I_1[kCnts]	284	±16	5.4%
A_2[kCnts/Chnl]	49.8	±3.3	6.5%
τ_2[ns]	1.149	±0.083	7.2%
I_2[kCnts]	1 787	±11	0.6%
A_3[kCnts/Chnl]	168.6	±5.3	3.1%
τ_3[ns]	0.215	±0.021	9.5%
I_3[kCnts]	1 131	±72	6.3%
A_4[kCnts/Chnl]	9.17	±0.75	8.1%
τ_4[ns]	4.81	±0.22	4.6%
I_4[kCnts]	1 378	±57	4.1%
$Bkgr_{Dec}$[kCnts]	0.0007	±0.0002	18%
$Bkgr_{IRF}$[Cnts/Chnl]	0.049	±0.024	49%
$Shift_{IRF}$[ps]	-27.6	±2.9	10%

b)

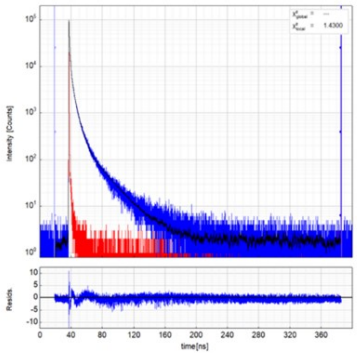

Parameter	Value	Δ	δ
A_1[kCnts/Chnl]	0.566	±0.064	11%
τ_1[ns]	24.24	±0.91	3.7%
I_1[kCnts]	429	±29	6.6%
A_2[kCnts/Chnl]	56.2	±3.0	5.3%
τ_2[ns]	1.513	±0.090	5.9%
I_2[kCnts]	2 652	±25	0.9%
A_3[kCnts/Chnl]	121.4	±2.2	1.7%
τ_3[ns]	0.303	±0.026	8.6%
I_3[kCnts]	1 150	±92	8.0%
A_4[kCnts/Chnl]	10.37	±1.00	9.6%
τ_4[ns]	5.77	±0.30	5.1%
I_4[kCnts]	1 867	±76	4.0%
$Bkgr_{Dec}$[kCnts]	0.0026	±0.0005	16%
$Bkgr_{IRF}$[Cnts/Chnl]	-0.045	±0.059	130%
$Shift_{IRF}$[ps]	-33.79	±0.60	1.8%

Figure S11. PL decay curves and their fits together with the tables with the fitted parameters for **NI1** in a) amorphous and b) crystalline state.

a)

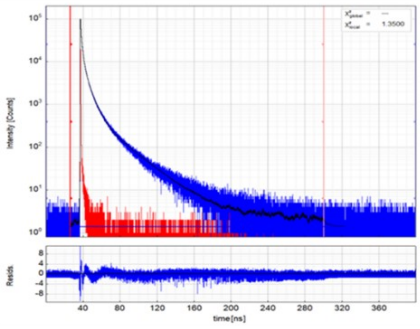

Parameter	Value	Δ	δ
A_1[kCnts/Chnl]	0.805	±0.027	3.3%
τ_1[ns]	24.99	±0.28	1.1%
I_1[kCnts]	1 257	±28	2.2%
A_2[kCnts/Chnl]	53.1	±1.2	2.2%
τ_2[ns]	1.615	±0.036	2.2%
I_2[kCnts]	5 355	±29	0.5%
A_3[kCnts/Chnl]	117.9	±1.5	1.2%
τ_3[ns]	0.304	±0.014	4.4%
I_3[kCnts]	2 236	±56	2.5%
A_4[kCnts/Chnl]	11.35	±0.32	2.7%
τ_4[ns]	6.10	±0.11	1.7%
I_4[kCnts]	4 324	±50	1.2%
$Bkgr_{Inst}$[kCnts]	0.0014	±0.0001	0.8%
$Bkgr_{IRF}$[Cnts/Chnl]	0.1453	±0.0051	3.4%
$Shift_{IRF}$[ps]	-31.2	±1.2	3.7%

b)

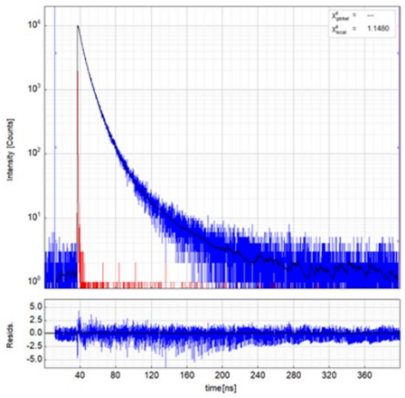

Parameter	Value	Δ	δ
A_1[kCnts/Chnl]	7.56	±0.22	2.9%
τ_1[ns]	4.989	±0.098	1.9%
I_1[kCnts]	589	±31	5.1%
A_2[kCnts/Chnl]	0.0928	±0.0078	8.3%
τ_2[ns]	42.5	±1.3	3.0%
I_2[kCnts]	61.6	±3.1	5.0%
A_3[kCnts/Chnl]	3.70	±0.22	5.7%
τ_3[ns]	11.61	±0.24	2.0%
I_3[kCnts]	670	±24	3.6%
$Bkgr_{Inst}$[kCnts]	0.0007	±0.0002	19%
$Bkgr_{IRF}$[Cnts/Chnl]	0.0024	±0.0049	204%
$Shift_{IRF}$[ps]	35.4	±1.7	4.6%

Figure S12. PL decay curves and their fits together with the tables with the fitted parameters for **NI2** in its a) amorphous and b) crystalline state.

6. Differential Scanning Calorimetry

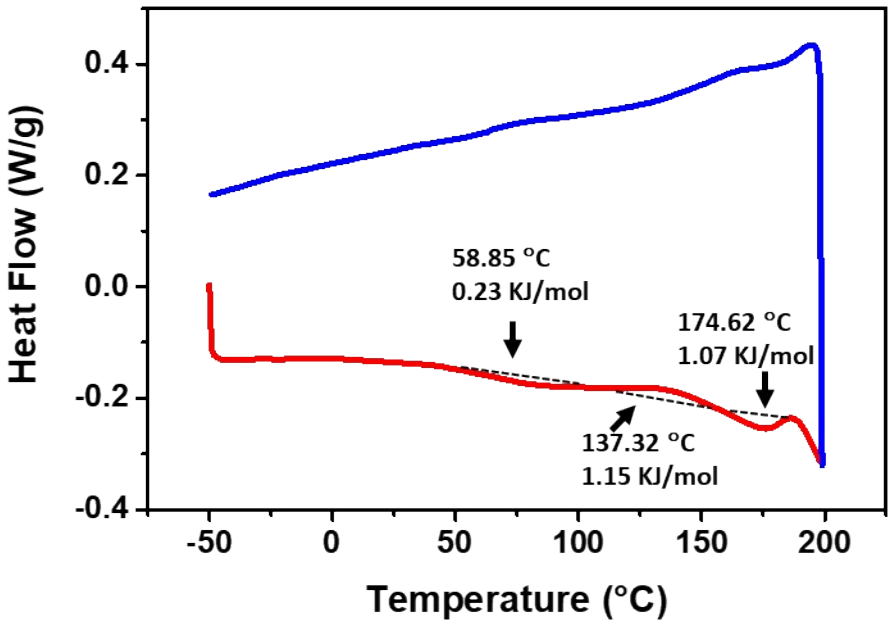

Figure S13. DSC curves for heating (red) and cooling (blue) of **NI1** measured at 10 °C/min. Exo up.

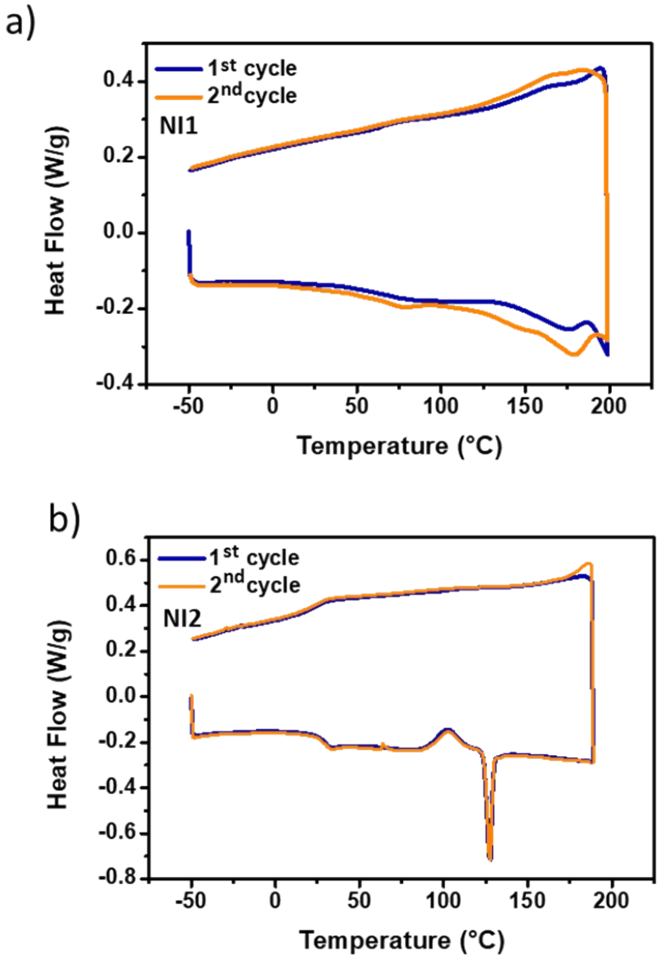

Figure S14. DSC curves for the first and second heating and cooling of a) **NI1** and b) **NI2** measured at 10 °C/min. Exo up.

7. Thermogravimetric analysis

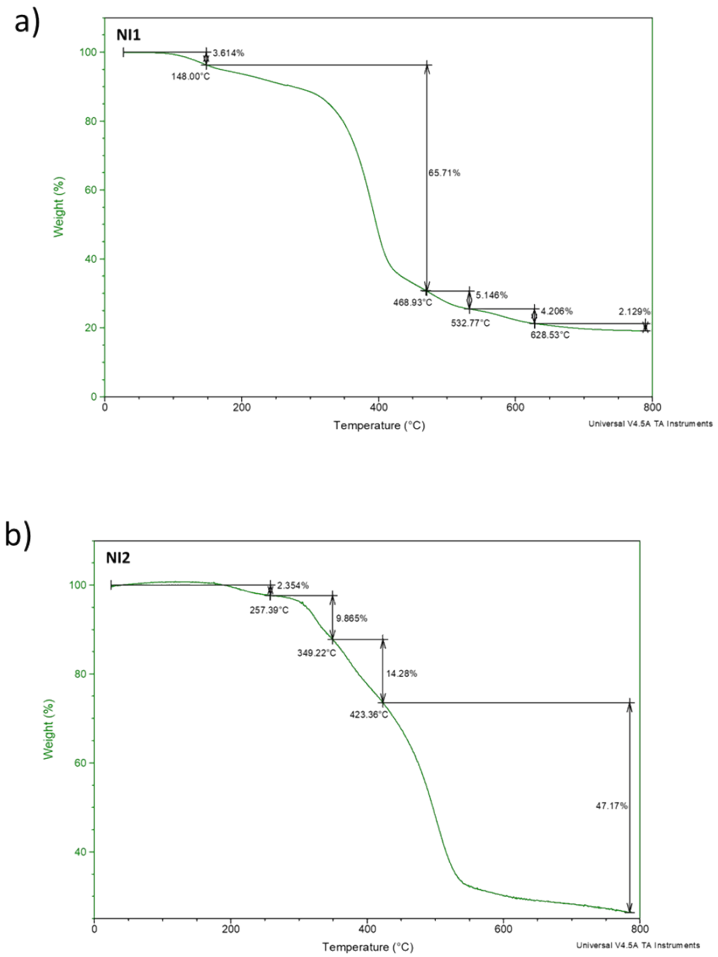

Figure S15. Thermogravimetric curves for a) **NI1** and b) **NI2** measured at nitrogen atmosphere.

8. Single crystal X-ray structure determination

8.1. Crystal Structure Report of NI1

Single crystals of $C_{40}H_{22}N_2O_2F_6$ (**NI1**) were solved. A suitable crystal was selected and placed on a MiTeGen micromount on a XtaLAB Synergy R, HyPix-Arc 100 diffractometer. The crystal was kept at 250.00(10) K during data collection. Using Olex2 [1], the structure was solved with the SHELXT [2] structure solution program using Intrinsic Phasing and refined with the SHELXL [3] refinement package using Least Squares minimisation.

Table S1. Crystal data and structure refinement of **NI1**

Chemical formula	$C_{40}H_{22}N_2O_2F_6$	
Formula weight /g/mol	676.59	
Temperature/K	250.00(10)	
Crystal size/mm³	0.187 × 0.022 × 0.016	
Crystal system	monoclinic	
Space group	$P2_1$	
Unit cell dimensions	a = 22.9998(13) Å	α = 90
	b = 4.7593(3) Å	β = 104.967(7)
	c = 31.222(2) Å	γ = 90
Volume/Å³	3301.7(4)	
Z	4	
Density (calculated) /g/cm³	1.361	
Absorption coefficient (μ)/mm⁻¹	0.915	
F(000)	1384.0	
Radiation	Cu Kα (λ = 1.54184)	
2Θ range for data collection/°	5.86 to 136.5	
Index ranges	-27 ≤ h ≤ 27, -5 ≤ k ≤ 5, -34 ≤ l ≤ 37	
Reflections collected	40752	
Independent reflections	11770 [Rint = 0.0949, Rsigma = 0.0818]	
Data/restraints/parameters	11770/881/875	
Goodness-of-fit on F²	1.035	
Final R indexes [I>=2σ (I)]	R1 = 0.1762, wR2 = 0.4394	
Final R indexes [all data]	R1 = 0.2832, wR2 = 0.5196	
Largest diff. peak/hole / e Å⁻³	1.05/-0.64	
Flack parameter	0.52(14)	

The crystal structure displays a high disorder in various parts of the two molecules contained in the asymmetric unit. This disorder has been modelled using geometrical restraints, and for atoms F1, F2, and F3, two sets of alternative positions (labeled A and B) have been located with respective occupancies of 54% and 46%. The presence of disorder and the existence of smaller domains together with the largest one, have contributed to a high wR2 value in the crystallographic analysis.

CCDC 2306089 for **NI1** contains the supplementary crystallographic data that can be obtained free of charge via www.ccdc.cam.ac.uk/data_request/cif, or by emailing

data_request@ccdc.cam.ac.uk, or by contacting The Cambridge Crystallographic Data Centre, 12 Union Road, Cambridge CB2 1EZ, UK; fax: +44 1223 336033.

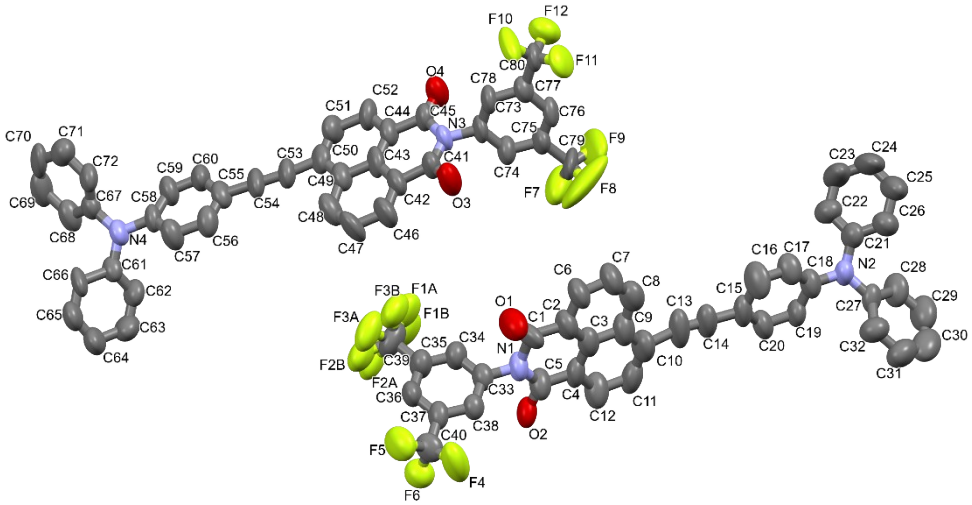

Figure S16. View of the two independent molecules of **NI1** in the asymmetric unit showing atom labelling and the atomic displacement parameters.

8.2. Crystal Structure Report of NI2

Single crystals of $C_{40}H_{36}N_2O_2$ (**NI2**) were solved. A suitable crystal was selected and placed on a MiTeGen micromount on a XtaLAB Synergy R, HyPix-Arc 100 diffractometer. The crystal was kept at 199.99(10) K during data collection. Using Olex2 [2], the structure was solved with the SHELXT [3] structure solution program using Intrinsic Phasing and refined with the SHELXL [4] refinement package using Least Squares minimisation.

Table S2. Crystal data and structure refinement of **NI2**

Chemical formula	$C_{40}H_{36}N_2O_2$
Formula weight /g/mol	576.71
Temperature/K	199.99(10)

Wavelength / Å	0.71073	
Crystal size /mm³	0.296 x 0.286 x 0.054	
Crystal system	monoclinic	
Space group	$P2_1/n$	
Unit cell dimensions	a = 9.64280(10) Å	α = 90°
	b = 41.4863(7) Å	β = 100.3360(10)°
	c = 15.9422(2) Å	γ = 90°
Volume /Å³	6274.09(15) Å³	
Z	8	
Density (calculated) /g/cm³	1.221	
Absorption coefficient (μ)/mm⁻¹	0.583	
F(000)	2448.0	
2Θ range for data collection/°	6.024 to 136.428°	
Index ranges	-11<=h<=11, -49<=k<=46, -19<=l<=14	
Reflections collected	59131	
Independent reflections	11446 [R(int) = 0.0242, R_{sigma}= 0.0198]	
Data / restraints / parameters	11446 / 86 / 795	
Goodness-of-fit on F²	1.028	
Final R indexes [I>=2σ (I)]	R1 = 0.0531, wR2 = 0.1532	
Final R indexes [all data]	R1 = 0.0599, wR2 = 0.1600	
Largest diff. peak and hole / e Å⁻³	0.386 and -0.394	

The crystal structure displays disorder for most of the atoms in one of the two molecules contained in the asymmetric unit. This disorder has been modelled using geometrical constraints with two sets of alternative positions (labeled A and B). Two variables were used for the disordered atoms: the ones located in the three-ring core present occupation factors of 76% (A) and 24% (B) and the ones in the aliphatic chain 60% (A) and 40% (B).

CCDC 2306088 for **NI2** contains the supplementary crystallographic data that can be obtained free of charge via www.ccdc.cam.ac.uk/data_request/cif, or by emailing data_request@ccdc.cam.ac.uk, or by contacting The Cambridge Crystallographic Data Centre, 12 Union Road, Cambridge CB2 1EZ, UK; fax: +44 1223 336033.

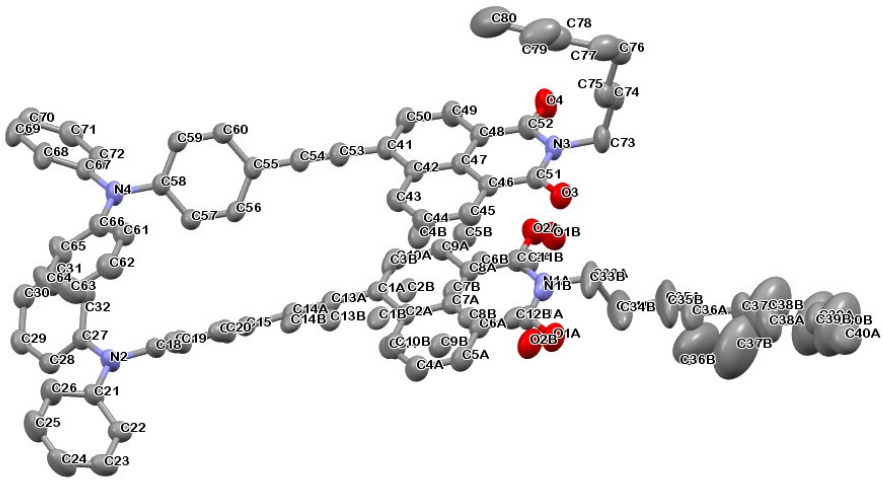

Figure S17. View of the two independent molecules of **NI2** in the asymmetric unit showing atom labelling and the atomic displacement parameters.

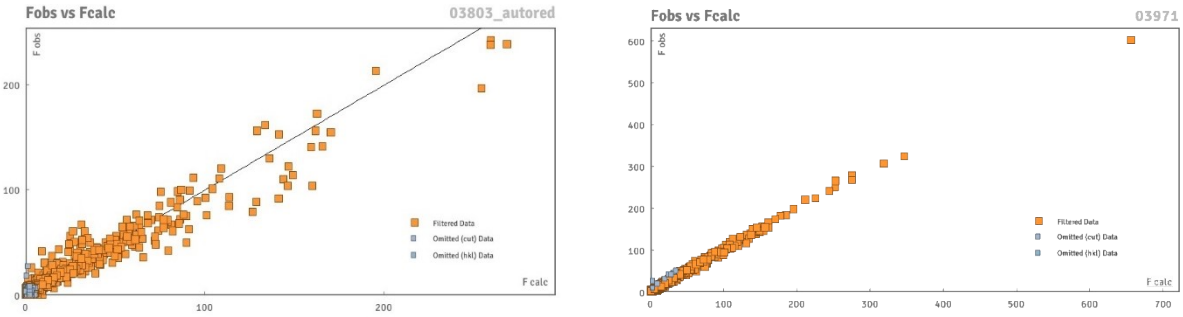

Figure S18. F_{obs} vs F_{calc} for **NI1** (left) and **NI2** (right).

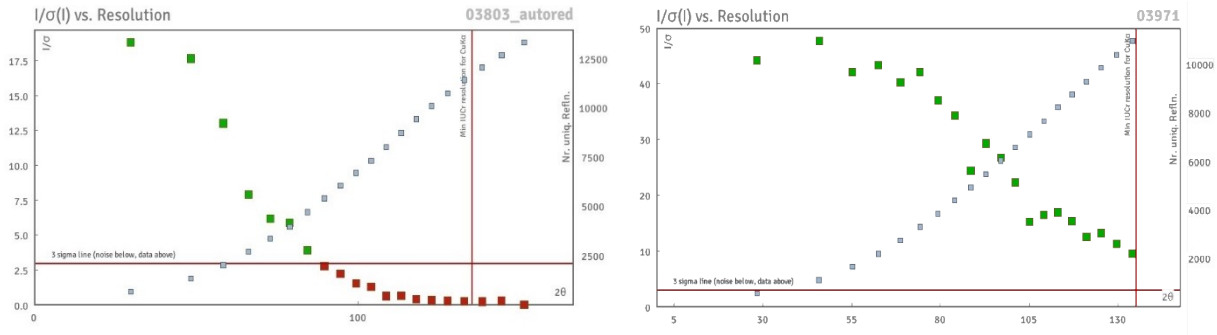

Figure S19. I/σ(I) vs resolution for **NI1** (left) and **NI2** (right).

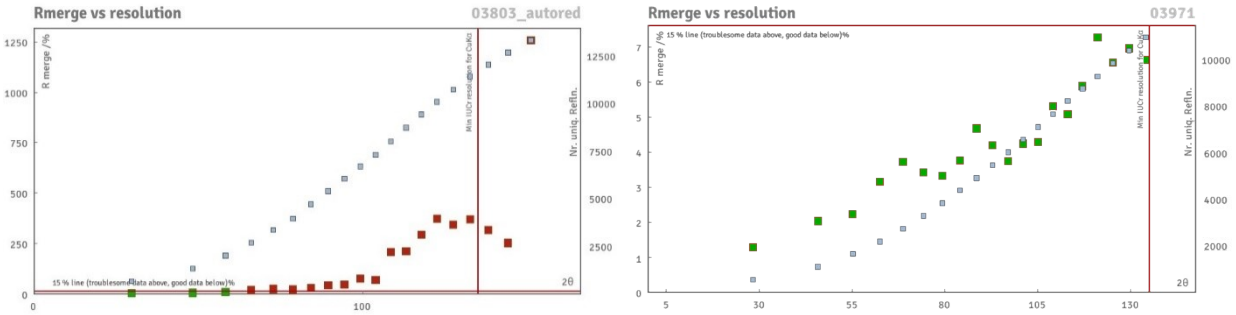

Figure S20. R_{merge} vs resolution for **NI1** (left) and **NI2** (right).

9. Powder X-ray analysis

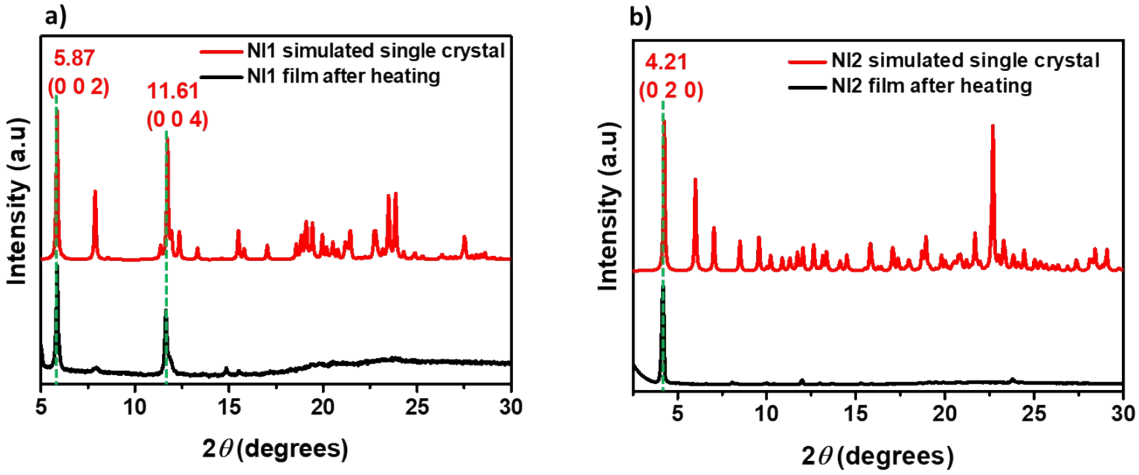

Figure S21. Comparison of powder X-ray diffraction patterns of simulated single crystal from crystal data determination and thin film layer after heating for a) **NI1** and b) **NI2**.

10. References

1. Lakowicz, J.R. Principles of Fluorescence Spectroscopy. 3rd Edition, Springer, Berlin. 2006.
2. Dolomanov, O.V. Bourhis, L.J., Gildea, R.J, Howard, J.A.K. and Puschmann, H. J. *Appl. Cryst*, 2009, **42**, 339-341.
3. Sheldrick, G. M. *Acta Cryst*. 2015 **A71**, 3-8.
4. Sheldrick, G. M. *Acta Cryst*., 2015 **C71**, 3-8.